

Research Paper

Entropy Analysis of a Variable Viscosity MHD Couette Flow Between Two Concentric Pipes with Convective Cooling

Oluwole Daniel MAKINDE¹⁾, Adetayo Samuel EEGUNJOBI^{2)*}

¹⁾ *Faculty of Military Science
Stellenbosch University*

Private Bag X2, Saldanha 7395, South Africa
e-mail: makinded@gmail.com

²⁾ *Mathematics Department
Namibia University of Science and Technology*

13 Jackson Kaujeua Street, Windhoek, Namibia

*Corresponding Author e-mail: samdet1@yahoo.com

This paper addresses the combined effects of the magnetic field, thermal buoyancy force, viscous dissipation, Joule heating and temperature-dependent viscosity on the Couette flow of an incompressible conducting fluid between two concentric vertical pipes. It is assumed that convective cooling occurs at the surface of the outer moving pipe while the surface of the inner fixed pipe is maintained at a constant temperature. The nonlinear equations for momentum and energy are obtained and solved numerically using a shooting method coupled with the Runge-Kutta-Fehlberg integration procedure. Relevant results depicting the effects of embedded thermophysical parameters on the velocity and temperature profiles, skin friction, the Nusselt number, entropy generation rate and the Bejan number are presented graphically and discussed. It is found that an increase in the magnetic field intensity boosts the entropy generation rate while an increase in convective cooling lessens it.

Key words: MHD; variable viscosity; Couette flow; concentric pipes; buoyancy force; heat transfer.

NOTATIONS

B_0 – radially imposed magnetic field,
 Be – Bejan number,
 Bi – thermal Biot number,
 b – outer pipe velocity parameter,
 Cf – skin friction,
 c_p – specific heat at constant pressure,
 Ec – Eckert number,
 E_G – volumetric entropy generation,

- Gr – Grashof number,
 g – acceleration due to gravity,
 h – heat transfer coefficient,
 k – fluid thermal conductivity,
 L – annulus gap parameter,
 m – material property,
 M – magnetic field parameter,
 N_1 – irreversibility due to heat transfer,
 N_2 – entropy generation due to viscous dissipation,
 N_s – dimensionless entropy generation rate,
 Nu – Nusselt number,
 P – fluid pressure,
 Pr – Prandtl number,
 r_1, r_2 – inner and outer pipes radii,
 r – radial distance,
 T – fluid temperature,
 T_0 – temperature at the inner pipe surface,
 T_a – ambient temperature,
 u – dimensional axial velocity,
 U – outer pipe velocity,
 w – dimensionless axial velocity,
 z – axial distance.

Greek Symbols

- μ_0 – fluid dynamic viscosity at the ambient temperature,
 μ – fluid dynamic viscosity,
 ρ – fluid density,
 β – volumetric thermal expansion coefficient,
 σ – fluid electrical conductivity,
 γ – rate of decrease in fluid viscosity due to temperature difference,
 η – dimensionless gap between two cylinders,
 β – volumetric thermal expansion coefficient,
 ε – dimensionless axial pressure gradient,
 θ – dimensionless temperature.

1. INTRODUCTION

Heat transfer within two concentric cylindrical pipes under Couette or Poiseuille flow scenarios can be found in many engineering and industrial processes that involve heating and cooling with the applications of heat exchangers. For instance, heat exchangers formed by concentric cylindrical pipes are widely used in space heating, refrigeration, air conditioning, power plant cooling, chemical

plants, petrochemical plants, petroleum refineries, natural gas processing, and sewage treatment. The continuous flow of heat-absorbing chilled liquid coolant within the concentric pipes prevents the heat accumulation within the inner pipe during operation. The fluid dynamics of a viscous liquid confined to the gap between two rotating cylinders have been theoretically and experimentally studied by many researchers [1, 2]. The exposure of the (electrically conductive) liquid to magnetic fields leads to a further improvement of flow process, which then relies on the geometry and strength of the magnetic field as well as the fluid's viscosity and resistivity ratio. The effect of aspect ratio on heat transfer flow through an annulus was researched by FÉNOT *et al.* [3]. Numerical study on thermal decomposition in a non-Newtonian reactive fluid flow within the annulus of a concentric cylindrical pipe under a generalized Couette flow was conducted by MAKINDE [4]. He obtained the critical values of exothermal reaction parameter for thermal stability in the flow systems were obtained. ATTIA [5] studied the effect of variable viscosity, magnetohydrodynamic (MHD), Joule and viscous dissipation of dusty fluid and heat transfer through parallel porous plates. He identified that the change in viscosity variation parameter leads to asymmetric velocity profiles about the central plane. MAKINDE and ONYEJEKWE [6] numerically studied the impact of variable viscosity and electrical conductivity on MHD generalized Couette flow with heat transfer characteristics. SETH *et al.* [7] studied the impacts of rotation and magnetic field on Couette flow of a viscous incompressible electrically conducting liquid in a rotating medium between two horizontal parallel porous plates. The magnetic field was found to have a tendency to retard fluid flow in both the main and secondary flow directions. ALI *et al.* [8] examined the effects of convective cooling on hydro-magnetic unsteady Couette flow of nanofluids and heat transfer in a rotating system. In the annular region between two coaxial circular tubes, SAMALAND BISWAL [9] researched the fluctuating flow of a second-order fluid. In the form of the Fourier series, they developed velocity components. The analytical and numerical solution for suddenly stopped axial Couette flow was researched by THIRUMARAN *et al.* [10]. They also took the stability flow into account when introducing a relatively small disturbance to the flow. The combined effects of Hall current, wall suction/injection and variable viscosity on Couette–Poiseuille flow of magnetic nanofluid through a rotating porous channel was investigated by MAKINDE *et al.* [11].

The present trend in optimizing the flow heat transfer is to evaluate the entropy generation rate in order to decrease its damaging impact on system efficiency. Thermodynamic irreversibility is expounded to entropy generation and occurs in all flow and heat transfer processes. In the flow and thermal systems, BEJAN [12] launched the theoretical assessment of the entropy generation rate. He showed that thermal system efficiency could be enhanced if the entropy gen-

eration could be minimized in the system. After his work, many researchers have conducted related analyses on completely different issues to examine the result of entropy generation on the thermal system and recommended means for minimizing the result. YURUSOY *et al.* [13] studied second law analysis in third-grade fluid flowing through a circular pipe with body dependent temperature. They identified that temperature within the rounded pipe decreased with the non-Newtonian parameter. The heat transfer and entropy generation within the flow of a variable consistency fluid through a cylindrical pipe with convective cooling was considered by TSHEHLA *et al.* [14]. They found that temperature distribution increases with increasing values of Brinkmann number. EEGUNJOBI and MAKINDE [15] numerically examined the entropy generation in Couette flow between two concentric pipes of variable viscosity fluid. They reported that the entropy generation rate increased with increasing of viscousness variation parameter. In a parallel composite channel with viscous and Joule heating, VYAS and RANJAN [16] studied generalized MHD Couette flow. They observed that the Bejan number rises with an upsurge in the temperature difference parameter. JAIN *et al.* [17] examined the thermodynamic study in generalized Couette flow through a porous medium with various heat boundary conditions, and discovered that the parameter of permeability improves the heat profiles. EEGUNJOBI and MAKINDE [18] considered the model of irreversibility and heat transfer on liquid film with magnetic force, buoyancy-driven variable viscosity and convective cooling. They noted that the profiles of Bejan numbers increase with increasing the Biot number. Several other authors [19–22] have considered entropy generation and its effects on various thermal flow configurations under various thermal boundary conditions.

The main objective of this study is to numerically investigate the combined effects of thermal buoyancy and variable viscosity on the inherent irreversibility in hydromagnetic Couette flow between two concentric pipes. In the following sections, the problem is formulated, analyzed and solved. Obtained results are presented graphically and discussed.

2. MATHEMATICAL MODEL

We consider a steady Couette flow of an incompressible, variable viscosity and electrically conducting fluid through the gap between two concentric vertical pipes under the combined action of thermal buoyancy, axial pressure gradient and radially imposed magnetic field of strength B_0 . The inner pipe is fixed while the outer pipe is subjected to uniform motion with velocity Ub in the axial direction. The surface of the inner pipe is maintained at uniform temperature T_0 , while the convective heat exchange with the ambient surrounding takes place at the surface of the outer pipe, as depicted in Fig. 1.

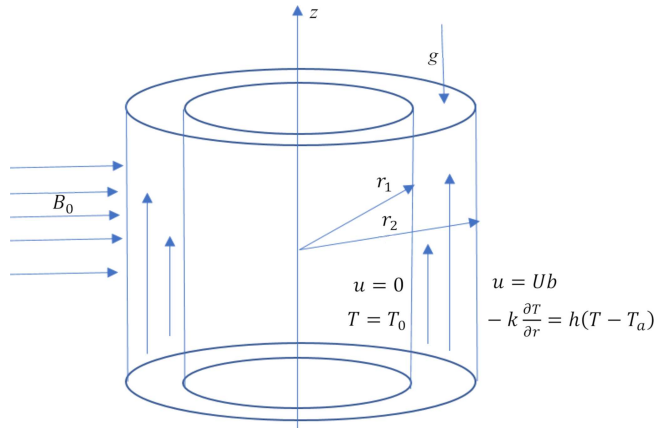


FIG. 1. Problem geometry.

The governing equations in the form presented by EGUNJOBI and MAKINDE [15] are given by

$$(2.1) \quad \frac{\partial u}{\partial z} = 0,$$

$$(2.2) \quad -\frac{\partial P}{\partial z} + \frac{1}{r} \frac{\partial}{\partial r} \left(r\mu(T) \frac{\partial u}{\partial r} \right) + g\beta(T - T_a) - \sigma B_0^2 u = 0,$$

$$(2.3) \quad \frac{k}{r} \frac{\partial}{\partial r} \left(r \frac{\partial T}{\partial r} \right) + \mu(T) \left(\frac{\partial u}{\partial r} \right)^2 + \sigma B_0^2 u^2 = 0,$$

$$(2.4) \quad E_G = \frac{k}{(T_0 - T_a)^2} \left[\frac{\partial T}{\partial r} \right]^2 + \frac{\mu(T)}{(T_0 - T_a)} \left[\frac{\partial u}{\partial r} \right]^2 + \frac{\sigma B_0^2 u^2}{(T_0 - T_a)}.$$

In addition to the concentric pipe flow, we write boundary conditions as follows:

$$(2.5) \quad \begin{aligned} u = 0, \quad T = T_0 \quad & \text{at } r = r_1, \\ u = Ub, \quad -k \frac{\partial T}{\partial r} = h(T - T_a) \quad & \text{at } r = r_2. \end{aligned}$$

The fluid temperature-dependent dynamical viscosity $\mu(T)$ is assumed to be

$$(2.6) \quad \mu(T) = \mu_0 e^{-m(T-T_a)},$$

where μ_0 is the fluid dynamic viscosity at the ambient temperature T_a such that $T_a < T_0$, m is material property, z is the axial distance, r is the radial distance, T is the fluid temperature, u is the axial velocity, r_1, r_2 are the inward and outward radii respectively, ρ is the fluid density, k is fluid thermal conductivity,

P is fluid pressure, β is volumetric thermal expansion coefficient, E_G is the volumetric entropy generation rate, g is the acceleration due to gravity, σ is the fluid electrical conductivity, and h is the heat transfer coefficient. The flow parameter b is defined such that $b = 0$ implies the Poiseuille flow scenario and $b > 0$ corresponds to generalized Couette flow. Using dimensionless variables

$$\begin{aligned}
 \bar{P} &= \frac{r_1 L P}{U \mu_0}, & w &= \frac{u}{U}, \\
 \eta &= \frac{r - r_1}{r_1 L}, & Z &= \frac{z}{r_1 L}, \\
 \theta &= \frac{T - T_1}{T_0 - T_1}, & L &= \frac{r_2 - r_1}{r_1}, \\
 (2.7) \quad \gamma &= m(T_0 - T_a), & M &= \frac{\sigma B_0^2 L^2 r_1^2}{\mu_0}, \\
 \text{Gr} &= \frac{g \beta r_1^2 L^2 (T_0 - T_a)}{U \mu_0}, & \text{Ns} &= \frac{E_g r_1^2 L^2}{k}, \\
 \text{Pr} &= \frac{\mu_0 c_p}{k}, & \text{Ec} &= \frac{U^2}{c_p (T_0 - T_a)}, \\
 \varepsilon &= -\frac{\partial \bar{P}}{\partial Z}, & \text{Bi} &= \frac{h r_1 L}{k},
 \end{aligned}$$

the dimensionless governing equations together with the appropriate boundary conditions can be written as

$$(2.8) \quad \frac{d^2 w}{d\eta^2} - \gamma \frac{dw}{d\eta} \frac{d\theta}{d\eta} + \left(\frac{L}{L\eta + 1} \right) \frac{dw}{d\eta} + (\text{Gr} \theta - Mw + \varepsilon) e^{\gamma\theta} = 0,$$

$$(2.9) \quad \frac{d^2 \theta}{d\eta^2} + \left(\frac{L}{L\eta + 1} \right) \frac{d\theta}{d\eta} + \text{Pr Ec} e^{-\gamma\theta} \left(\frac{dw}{d\eta} \right)^2 + M \text{Pr Ec} w^2 = 0,$$

$$(2.10) \quad \text{Ns} = \left[\frac{dw}{d\eta} \right]^2 + \text{Pr Ec} e^{-\gamma\theta} \left[\frac{dw}{d\eta} \right]^2 + M \text{Pr Ec} w^2,$$

with

$$(2.11) \quad w(0) = 0, \quad \theta(0) = 1, \quad w(1) = b, \quad \frac{d\theta}{d\eta}(1) = -\text{Bi} \theta(1),$$

where γ is the rate of decrease in fluid viscosity due to temperature difference, M is the magnetic field parameter, ε is the pressure gradient parameter, Gr is the

Grashof number, C_p is the specific heat at constant pressure, L is the concentric cylinders gap parameter, Pr is the Prandtl number, Ec is the Eckert number, Bi is the thermal Biot number, and η is the dimensionless gap between the two cylinders. Other parameters of interest are the skin friction (Cf) and the Nusselt number (Nu), and they are defined as

$$(2.12) \quad Cf = \frac{r_1 L \tau}{\mu_0 U} = e^{-\gamma \theta(\eta)} \left. \frac{dw(\eta)}{d\eta} \right|_{\eta=0,1}, \quad Nu = \frac{r_1 L q}{k(T_0 - T_a)} = - \left. \frac{d\theta(\eta)}{d\eta} \right|_{\eta=0,1},$$

where

$$\tau = \mu(T) \left. \frac{du}{dr} \right|_{r_1, r_2} \quad q = -k \left. \frac{dT}{dr} \right|_{r_1 r_2}.$$

The Bejan number (Be) is defined as

$$(2.13) \quad Be = \frac{N_1}{N_s} = \frac{N_1}{N_1 + N_2},$$

where $N_2 = Pr Ec e^{-\gamma \theta} \left[\frac{dw}{d\eta} \right]^2 + M Pr Ec w^2$ is the entropy generation due to viscous dissipation and magnetic field, $N_1 = \left[\frac{d\theta}{d\eta} \right]^2$ is the irreversibility due to heat transfer.

3. NUMERICAL PROCEDURE

The nonlinear boundary value problem described by model Eqs (2.8)–(2.11) is numerically tackled using a shooting method coupled with the Runge-Kutta-Fehlberg integration scheme [23]. Let

$$(3.1) \quad w = y_1, \quad w' = y_2, \quad \theta = y_3, \quad \theta' = y_4.$$

The governing equations are then transformed into a set on nonlinear initial value problem as

$$(3.2) \quad \left. \begin{aligned} y_1' &= y_2 \\ y_2' &= \gamma y_2 y_4 - \left(\frac{L}{L\eta+1} \right) y_2 + (M y_1 - Gr y_3 - \varepsilon) e^{\gamma y_3} \\ y_3' &= y_4 \\ y_4' &= - \left(\frac{L}{L\eta+1} \right) y_4 - Pr Ec e^{-\gamma \theta} y_2^2 - M Pr Ec y_1^2 \end{aligned} \right\}$$

with the corresponding initial conditions given as

$$(3.3) \quad y_1(0) = 0, \quad y_2(0) = a_1, \quad y_3(0) = 1, \quad y_4(0) = a_2.$$

The unknown initial values of a_1 and a_2 in Eq. (3.3) are first estimated and after that determined accurately using a shooting method with the Newton-Raphson's iteration technique with a step size of $\Delta\eta = 0.01$. Numerical solutions obtained for the velocity and temperature profiles are used to compute the values for the skin friction, the Nusselt number, the entropy generation rate and the Bejan number as specified in Eqs (2.12) and (2.13).

4. RESULTS AND DISCUSSION

The dimensionless fluid velocity, the temperature, the skin friction, the Nusselt number, the entropy generation rate, and the Bejan number are presented in Figs 2–27 for various essential physical parameters. The variation of the fluid velocity profiles in the annulus within the concentric pipes is depicted in Figs 2–6.

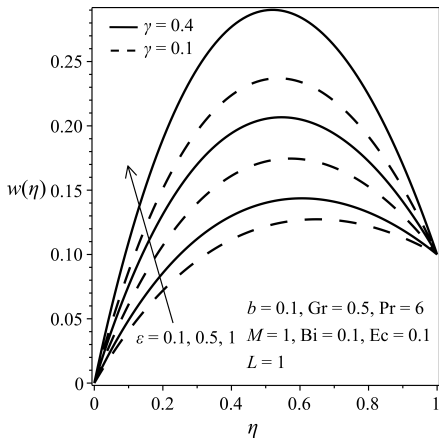


FIG. 2. Impact of γ and ϵ on $w(\eta)$.

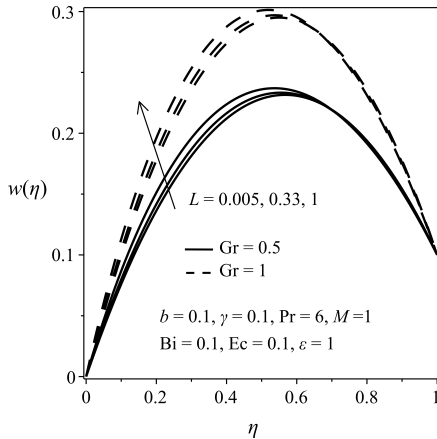


FIG. 3. Impact of Gr and L on $w(\eta)$.

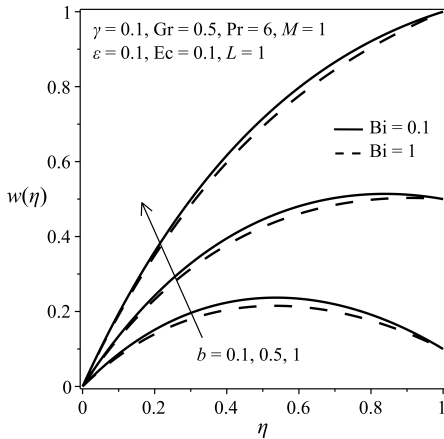


FIG. 4. Impact of b and Bi on $w(\eta)$.

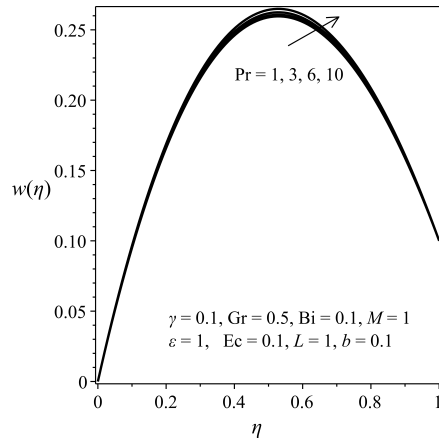


FIG. 5. Impact of Pr on $w(\eta)$.

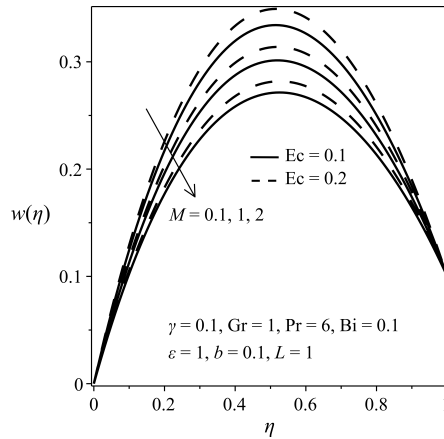


FIG. 6. Impact of M and Ec on $w(\eta)$.

In general, the fluid velocity is zero at the surface of the inner fixed pipe due to no-slip condition, while it increases gradually to its maximum value within the annulus and then slightly declines to the prescribed outer moving pipe velocity. An increase in axial pressure gradient parameter (ε) and variable viscosity (γ) parameter increases the fluid velocity, as shown in Fig. 2. A similar trend of enhanced velocity is noticed in Figs 3–6 with a rise in the Grashof number (Gr), the Eckert number (Ec), the annulus gap parameter (L), the outer pipe motion parameter (b) and the Prandtl number (Pr). However, the trend is reversed with a decline in velocity profiles as the value of the magnetic field parameter (M) and thermal Biot number (Bi) increases. This may be attributed to the fact that as parameter values ε , γ , Gr , Ec , L , and Pr increase, the fluid viscosity decreases due to a rise in temperature while the annulus gap between the two pipes widens, consequently resulting in an increase in the flow rate. Meanwhile, the flow rate decreases with a rise in parameter values of Bi and M due to the combined effects of convective cooling at the surface of the outer moving pipe and the presence of the Lorentz force that tends to slow down the conducting fluid motion.

The effects of various thermophysical parameters on the fluid temperature profiles are displayed in Figs 7–11. Generally, the fluid temperature within the concentric pipe annulus is greatly influenced by the rate of convective heat loss to the ambient surrounding at the outer pipe surface. Interestingly, an increase in the fluid temperature is observed with increasing parameter values of ε , γ , Gr , b , Ec , M , and Pr . Moreover, as the values of these parameters increase, the fluid viscosity decreases due to thermal buoyancy while the flow rate increases, and consequently, the rate of internal heat generation due to viscous dissipation and the Joule heating intensifies and the fluid temperature is enhanced.

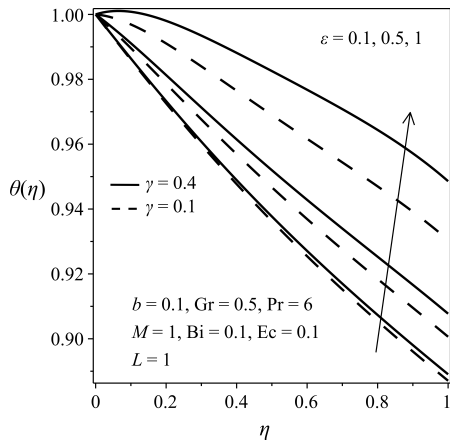


FIG. 7. Impact of ε and γ on $\theta(\eta)$.

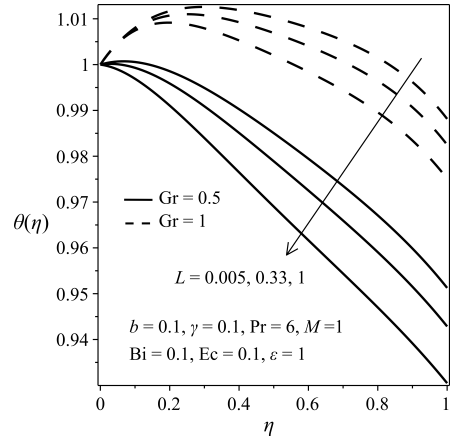


FIG. 8. Impact of Gr and L on $\theta(\eta)$.

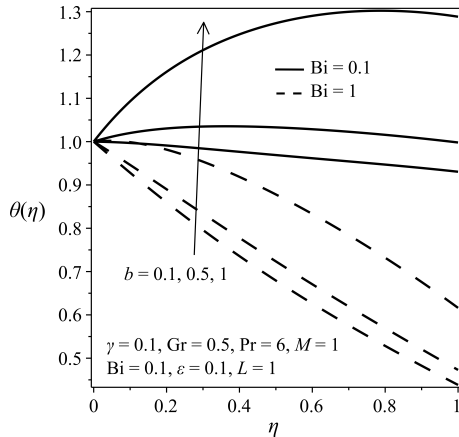


FIG. 9. Impact of b and Bi on $\theta(\eta)$.

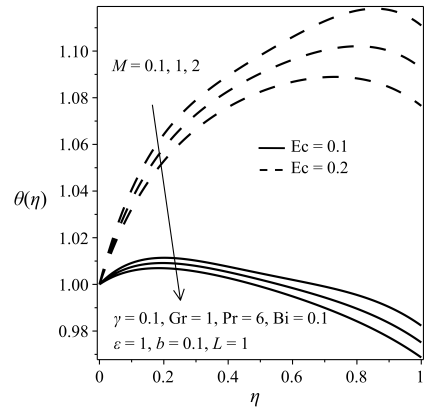


FIG. 10. Impact of M and Ec on $\theta(\eta)$.

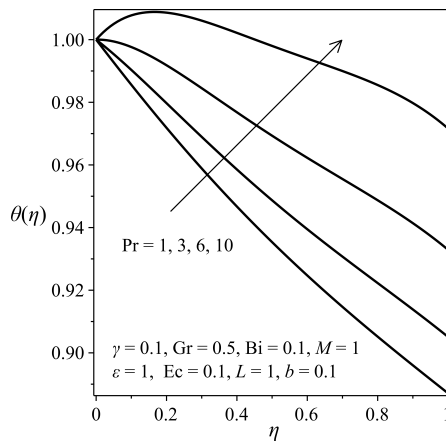


FIG. 11. Impact of Pr on $\theta(\eta)$.

Meanwhile, the trend is opposite with the fluid temperature decreasing as the parameter values of Bi and L increase. This is expected as an increase in Bi leads to an increase in the rate of convecting cooling at the outer moving pipe surface. Additionally, an increase in L widens the concentric pipes annulus, which invariably reduces the frictional heating and the fluid temperature falls.

The effects of various embedded parameters on the skin friction and Nusselt number are depicted in Figs 12–17. It is noteworthy to mention that the skin friction at the inner surface of the outer moving pipe grows rapidly with an increase in the parameter values of ε , γ , Gr , Ec , L , and Pr , as illustrated in Figs 12–14. This can be attributed to the fact that the fluid becomes lighter as a result of a decrease in viscosity caused by thermal buoyancy. The flow rate is enhanced due to a widening gap of the concentric pipes annulus, and consequently, the velocity gradient at the inner surface of the outer moving pipe

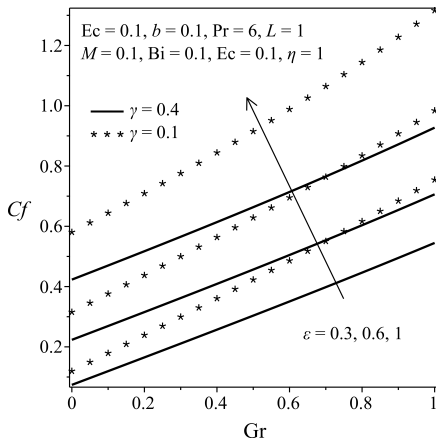


FIG. 12. Impact of ε , Gr and γ on Cf .

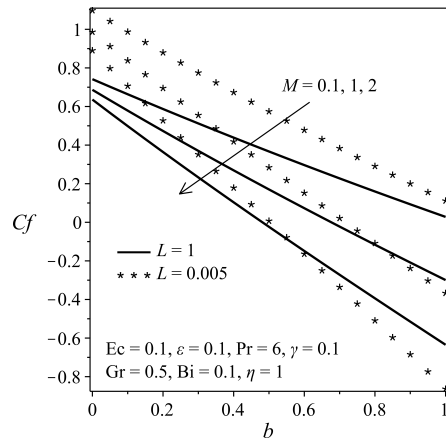


FIG. 13. Impact of b , L and M on Cf .

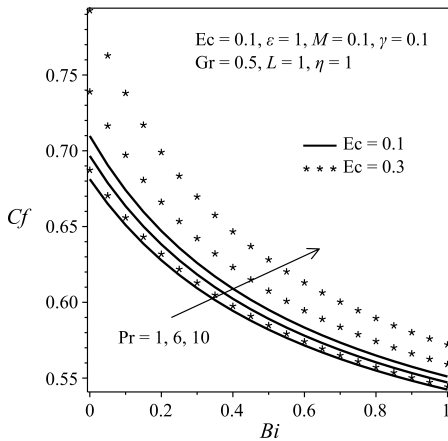


FIG. 14. Impact of Bi , Ec and Pr on Cf .

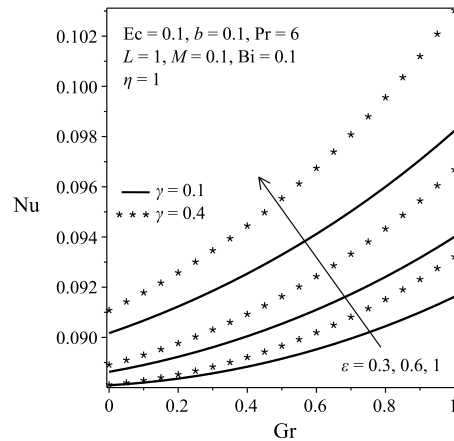
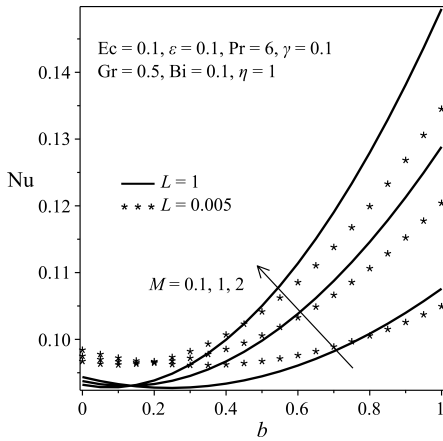
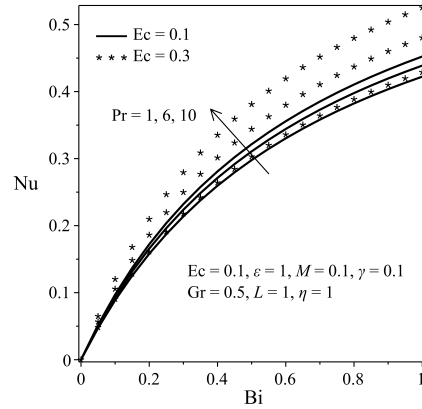


FIG. 15. Impact of ε , Gr and γ on Nu .

FIG. 16. Impact of b , L and M on Nu .FIG. 17. Effects of Bi , Ec and Pr on Nu .

is enhanced. Meanwhile, an increase in the parameter values of M , b , and Bi reduces the skin friction. This is expected as the rise in magnetic field intensity tends to slow down the flow rate, which invariably diminishes the shear stress at the inner surface of the outer moving pipe. Similarly, as the convective heat loss rises, the fluid viscosity increases and the flow rate drops. Consequently, the velocity gradient at the outer moving pipe is reduced. It is noteworthy to mention that the flow separation and flow reversal denoted by zero and the negative skin friction may occur in the flow field with a decrease in the annulus gap and a boost in the outer pipe surface motion. In Figs 15–17, we observed that the heat transfer rate at the outer moving pipe escalates with an increase in the parameter values of ε , γ , Pr , M , Bi , L , Gr , b , and Ec . The rise in the Nusselt number can be ascribed to an increase in temperature gradient at the outer moving pipe due to the combined action of convective cooling, viscous dissipation, thermal buoyancy and the Joule heating.

Figures 18–22 show the effects of thermophysical parameters on the entropy generation rate. Generally, the entropy generation rate near the fixed inner pipe region is higher than that generated near the outer moving pipe. The lowest entropy production is observed at the core region of the annulus gap. A rise in parameter values of ε , γ , Gr , L , b , and Ec boosts the entropy production in the flow system. This increase in the entropy generation rate is caused by the increased velocity and temperature gradients within the flow system due to combined effects of thermal buoyancy, annulus gap widening coupled with increasing flow rate and a decrease in fluid viscosity. Notably, the efficiency of the flow system may be adversely affected by the high rate of entropy production under the scenario of these parameter values. Interestingly, the entropy generation rate declines with an increase in magnetic field intensity (M) and convective cooling

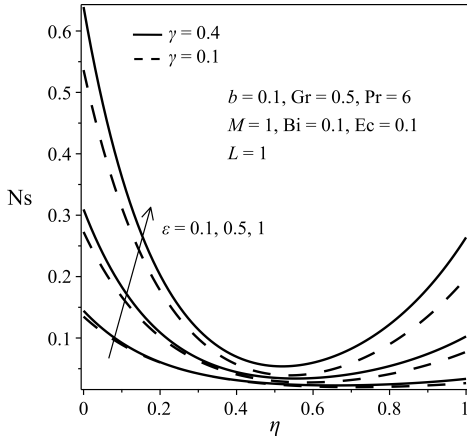


FIG. 18. Impact of γ and ϵ on N_s .

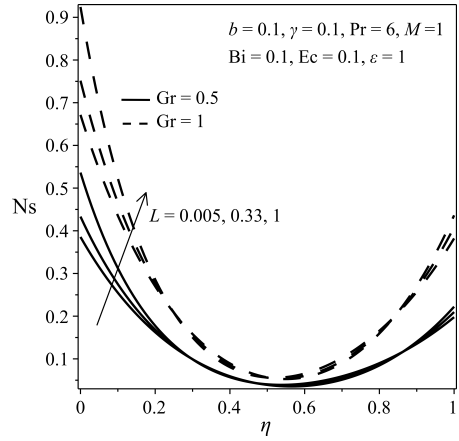


FIG. 19. Impact of Gr and L on N_s .

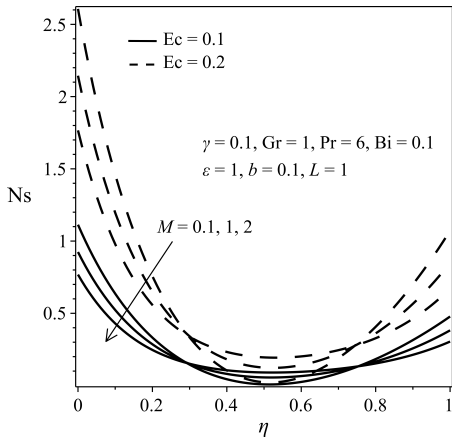


FIG. 20. Impact of M and Ec on N_s .

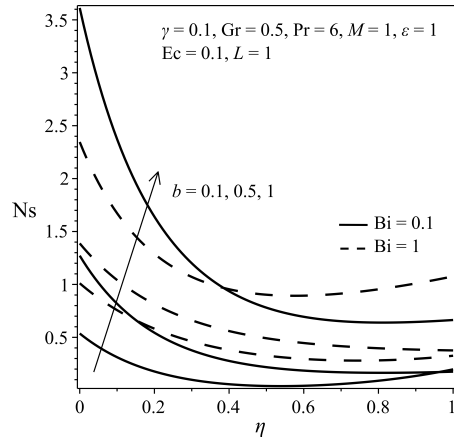


FIG. 21. Impact of b and Bi on N_s .

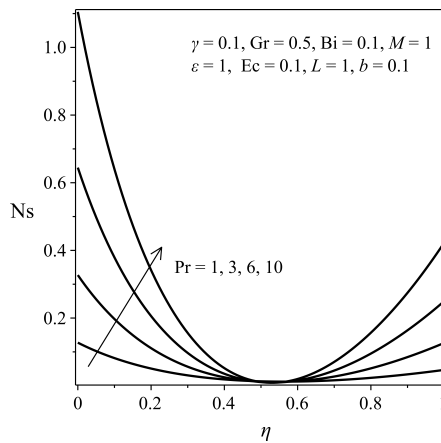


FIG. 22. Impact of Pr on N_s .

(Bi) at the outer moving pipe surface, as shown in Figs 20 and 21. This reduction in entropy production may be attributed to a convective heat loss to the ambient surrounding and a drop in the flow rate, which invariably lower the velocity and temperature gradients within the flow system.

Figures 23–27 present the effects of some of the physical parameters on the Bejan number. In all the figures, the Bejan number attained its maximum value at the core region of the concentric pipes annulus. This implies that the contribution of heat transfer irreversibility to the overall entropy generation is higher at this core region, while the irreversibility due to the fluid friction and magnetic field dominates at the pipe’s inner surface. Moreover, the Bejan number increases with increasing annulus gap (L), viscous heating (Ec) and convective cooling (Bi) at the outer moving pipe but lessens with a rise in parameter values of ε , γ , Gr, M , and Pr. The rise in the Bejan number as parameter values of L ,

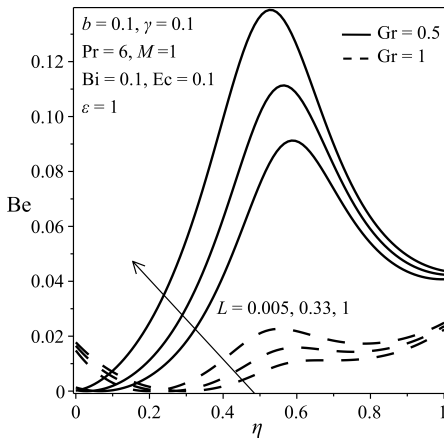


FIG. 23. Impact of Gr and L on Be.

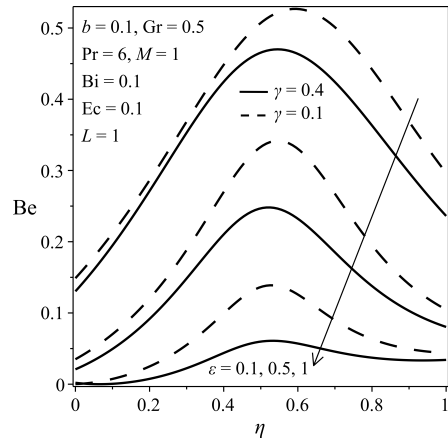


FIG. 24. Impact of γ and ε on Be.

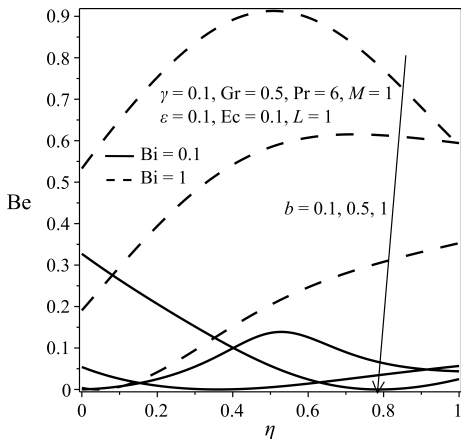


FIG. 25. Impact of b and Bi on Be.

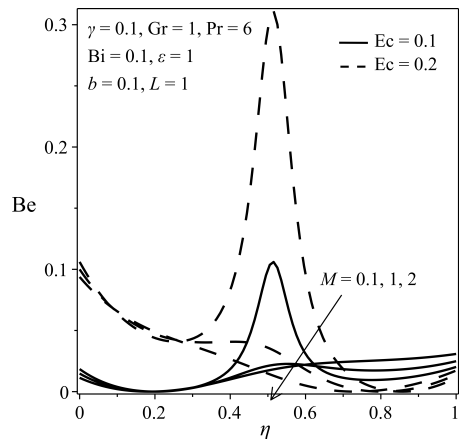


FIG. 26. Impact of M and Ec on Be.

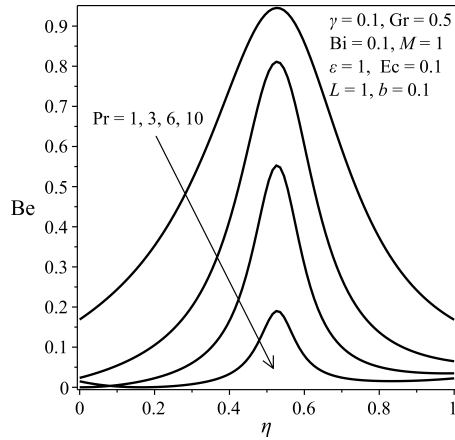


FIG. 27. Impact of Pr on Be.

Ec, and Bi increase can be attributed to the growing influence of heat transfer irreversibility on the entropy generation rate. By contrast, a reduction in the Bejan number as parameter values of ε , γ , Gr, M , and b rise, depicts the prevailing effect of viscous dissipation and Joule heating irreversibility on the total entropy production in the flow system. Moreover, we observed that for very low Prandtl number (Pr) fluid, the dominance of heat transfer irreversibility is absolute at the core region of the concentric pipes annulus, while for high Prandtl fluid, the irreversibility due to fluid friction and magnetic field completely dominates the annulus core region, as shown in Fig. 27. With appropriate regulation of these parameter values, the entropy generation rate due to heat transfer, viscous dissipation and Joule heating can be minimized for the efficient operation of the flow system.

5. CONCLUSIONS

In this investigation, the magnetohydrodynamics with heat transfer and entropy generation rate in a Couette flow of a conducting variable viscosity fluid within the annulus between two concentric vertical pipes was analyzed. The governing differential equations were solved numerically using the shooting method coupled with the Runge-Kutta-Fehlberg integration procedure. The obtained results can be summarized as follows:

- Fluid velocity profiles were enhanced with a rise in parameter values of ε , γ , Gr, L , Ec, b , and Pr but declined with a rise in M and Bi.
- An increase in parameter values of ε , γ , Gr, b , Ec, M , and Pr increased the temperature profiles while an increase in Bi and L decreased these profiles.

- The skin friction at the outer moving pipe increased with an increase in the parameter values of ε , γ , Gr, Ec, L , and Pr but decreased with a rise in M , b , and Bi.
- The Nusselt number at the outer moving pipe enhanced with an increase in the parameter values of ε , γ , Pr, M , Bi, L , Gr, b , and Ec.
- A rise in parameter values of ε , γ , Gr, L , b , and Ec boosted the entropy generation rate while a rise in Bi and M lessened it.
- The Bejan number lessened with an increase in parameter values of ε , γ , Gr, M , and b ; however it amplified with a rise in parameter values of L , Ec, and Bi. The dominant effects of viscous dissipation and Joule heating irreversibility were more pronounced near the walls of the concentric pipes walls while the heat transfer irreversibility effects prevailed at the annulus core region.

Finally, it is anticipated that with the appropriate adjustment of the emerging thermophysical parameters, both the flow and heat transfer rate can be further enhanced while the entropy generation rate is minimized. This may invariably enhance the optimum design and performance of concentric pipe heat exchangers.

REFERENCES

1. MARON D.M., COHEN S., Hydrodynamics and heat/mass transfer near rotating surfaces, *Advances in Heat Transfer*, **21**: 141–183, 1992, doi: 10.1016/S0065-2717(08)70335-6.
2. WATANABE T., TOYA Y., NAKAMURA I., Development of free surface flow between concentric cylinders with vertical axes, *Journal of Physics: Conference Series*, **14**(1): 9–19, 2005, doi: 10.1088/1742-6596/14/1/002.
3. FÉNOT M., BERTIN Y., DORIGNAC E., LALIZEL G., A review of heat transfer between concentric rotating cylinders with or without axial flow, *International Journal of Thermal Sciences*, **50**(7): 1138–1155, 2011, doi: 10.1016/j.ijthermalsci.2011.02.013.
4. MAKINDE O.D., Thermal analysis of a reactive generalized Couette flow of power law fluids between concentric cylindrical pipes, *The European Physical Journal Plus*, **129**(12): Article ID: 270 (9 pages), 2014, doi: 10.1140/epjp/i2014-14270-4.
5. ATTIA H., Influence of temperature-dependent viscosity on the MHD Couette flow of dusty fluid with heat transfer, *International Journal of Differential Equations*, **2006**: Article ID: 75290 (14 pages), 2006, doi: 10.1155/DENM/2006/75290.
6. MAKINDE O.D., ONYEJEKWE O.O., A numerical study of MHD generalized Couette flow and heat transfer with variable viscosity and electrical conductivity, *Journal of Magnetism and Magnetic Materials*, **323**(22): 2757–2763, 2011, doi: 10.1016/j.jmmm.2011.05.040.
7. SETH G.S., ANSARI MD.S., NANDKEOLYAR R., Effects of rotation and magnetic field on unsteady Couette flow in a porous channel, *Journal of Applied Fluid Mechanics*, **4**(2): 95–103, 2011.

8. ALI A.O., MAKINDE O.D., NKANSAH-GYEKYE Y., Numerical study of unsteady MHD Couette flow and heat transfer of nanofluids in a rotating system with convective cooling, *International Journal of Numerical Methods for Heat & Fluid Flow*, **26**(5): 1567–1579, 2016, doi: 10.1108/HFF-10-2014-0316.
9. SAMAL R.C., BISWAL T., Fluctuating flow of a second order fluid between two co-axial circular pipes, *International Journal of Engineering Research & Technology (IJERT)*, **4**(2): 433–441, 2015.
10. THIRUMARAN V., WELIWITA J.A., ISHAK M.I.M., An analysis of axial Couette flow in annular region of abruptly stopped pipes, *Physical Science International Journal*, **17**(4): 1–12, 2018, doi: 10.9734/PSIJ/2018/40076.
11. MAKINDE O.D., ISKANDER T., MABOOD F., KHAN W.A., TSHEHLA M.S., MHD Couette-Poiseuille flow of variable viscosity nanofluids in a rotating permeable channel with Hall effects, *Journal of Molecular Liquids*, **221**: 778–787, 2016, doi: 10.1016/j.molliq.2016.06.037.
12. BEJAN A., Second-law analysis in heat transfer and thermal design, *Advance in Heat Transfer*, **15**: 1–58, 1982, doi: 10.1016/S0065-2717(08)70172-2.
13. YÜRÜSOY M., YILBAS B.S., PAKDEMIRLI M., Non-Newtonian fluid flow in annular pipes and entropy generation: Temperature-dependent viscosity, *Sadhana*, **31**(6): 683–695, 2006, doi: 10.1007/BF02716888.
14. TSHEHLA M.S., MAKINDE O.D., OKECHA G.E., Heat transfer and entropy generation in a pipe flow with temperature dependent viscosity and convective cooling, *Scientific Research and Essays*, **5**(23): 3730–3741, 2010.
15. EEGUNJOBI A.S., MAKINDE O.D., Entropy generation analysis in transient variable viscosity Couette flow between two concentric pipes, *Journal of Thermal Science and Technology*, **9**(2): 1–11, 2014, doi: 10.1299/jtst.2014jtst0008.
16. VYAS P., RANJAN A., Entropy analysis for MHD generalised Couette flow in a composite duct, *Journal of Industrial Mathematics*, **2015**, Article ID: 895046 (10 pages), 2015, doi: 10.1155/2015/895046.
17. JAIN S., KUMAR V., BOHRA S., Entropy generation in generalized Couette flow through porous medium with different thermal boundary conditions, *International Journal of Energy & Technology*, **7**: 40–48, 2015, doi: 10.1155/2015/895046.
18. EEGUNJOBI A.S., MAKINDE O.D., Irreversibility analysis of MHD buoyancy-driven variable viscosity liquid film along an inclined heated plate with convective cooling, *Journal of Applied and Computational Mechanics*, **5**(5): 840–848, 2019, doi: 10.22055/jacm.2019.28313.1476.
19. MKWIZU M.H., MAKINDE O.D., NKANSAH-GYEKYE Y., Numerical investigation into entropy generation in a transient generalized Couette flow of nanofluids with convective cooling, *Sadhana*, **40**(7): 2073–2093, 2015, doi: 10.1007/s12046-015-0432-0.
20. MAKINDE O.D., EEGUNJOBI A.S., TSHEHLA M.S., Thermodynamics analysis of variable viscosity hydromagnetic Couette flow in a rotating system with Hall effects, *Entropy*, **17**(11): 7811–7826, 2015, doi: 10.3390/e17117811.

21. EEGUNJOBI A.S., MAKINDE O.D., TSHEHLA M.S., FRANKS O., Irreversibility analysis of unsteady Couette flow with variable viscosity, *Journal of Hydrodynamics*, **27**(2): 304–310, 2015, doi: 10.1016/S1001-6058(15)60485-1.
22. MAKINDE O.D., FRANKS O., Thermal decomposition of unsteady non-Newtonian MHD Couette flow with variable properties, *International Journal of Numerical Methods for Heat & Fluid Flow*, **25**(2): 252–264, 2015, doi: 10.1108/HFF-12-2013-0342.
23. CEBECI T., BRADSHAW P., *Physical and computational aspects of convective heat transfer*, New York, USA, Springer, 1988.

Received September 24, 2019; accepted version May 24, 2020.

Published on Creative Common licence CC BY-SA 4.0

